

Cardiovascular Signal Decomposition and Estimation with the Extended Kalman Smoother

James McNames and Mateo Aboy

Abstract— Cardiovascular signals such as arterial blood pressure (ABP), pulse oximetry (S_pO_2), and central venous pressure (CVP) contain useful information such as heart rate, respiratory rate, and pulse pressure variation (PPV). We present a statistical state-space model of cardiovascular signals that can be used with the extended Kalman filter or smoother to simultaneously estimate and track many cardiovascular parameters of interest. We demonstrate the algorithm's tracking capabilities with a real ABP signal.

I. INTRODUCTION

Accurate estimation and tracking of the heart and respiratory frequencies from ABP, S_pO_2 , and CVP is important for algorithms embedded in patient monitors in the emergency room and intensive care applications. Commercial monitoring systems often include the capability to monitor heart rate, systolic, diastolic, and mean pressures, but few can reliably estimate other components of pressure waveforms such as the respiratory rate, pulse pressure variation, or pulse morphology.

Pulse pressure variation (PPV) is a form of amplitude modulation of the pressure waveform due to intrathoracic pressure fluctuations that occur with respiration. Numerous studies have found that PPV is one of the most sensitive and specific predictors of fluid responsiveness, and it is used to guide fluid therapy in multiple patient populations receiving mechanical ventilation [1]–[5]. Currently, there are few publicly available algorithms capable of estimating PPV [6]. Thus, researchers need to rely on commercial devices such as the PiCCO[®] system (Pulsion Medical Systems, Munich, Germany), which use proprietary algorithms for PPV estimation.

We propose a statistical state-space model of cardiovascular signals that is designed for use with the extended Kalman filter and smoother to estimate and track all the model parameters of interest including the cardiac fundamental frequency and higher harmonics, respiratory fundamental frequency and higher harmonics, cardiac component harmonic amplitudes and phases, respiratory component harmonic amplitudes and phases, and degree of PPV.

This work was supported by the Thrasher Research Fund.

J. McNames is director of the Biomedical Signal Processing Laboratory and an associate professor of the Department of Electrical and Computer Engineering at Portland State University, Portland, Oregon. Email: mcnames@pdx.edu.

M. Aboy is a member of the Biomedical Signal Processing Laboratory at Portland State University and an assistant professor at the Oregon Institute of Technology, Beaverton, Oregon. Email: mateoaboy@ieee.org

II. ALGORITHM DESIGN

The Kalman filter recursively estimates the state of a linear stochastic process such that the mean squared error is minimized [7]. The Kalman smoother is a noncausal estimator that uses the entire record to estimate the state of a linear stochastic process. The extended versions of the Kalman filter and smoother are generalizations to the case of a nonlinear state space model that use a local linear approximation of the model. Since each updated estimate of the state is computed based on the previous state and the current values of the observed signal, the storage and computational requirements are manageable for most applications.

A. Statistical Model of the Observed Signal

Our statistical model of cardiovascular signals consists of three primary components: $m(n)$, the low-frequency signal trend; $y_r(n)$, a quasi-periodic respiratory signal with a fundamental frequency equal to the respiratory rate; $y_c(n)$, a quasi-periodic cardiac signal with a fundamental frequency equal to the heart rate; and $v(n)$, a white noise signal that accounts for the variation that is not explained by the other three components. The respiratory component $y_r(n)$ is present in the signal additively and through amplitude modulation of the cardiac component. More precisely, our statistical model of the cardiovascular signal is

$$y(n) = m(n) + y_r(n) + [1 + \rho(n)y_r(n)]y_c(n) + v(n) \quad (1)$$

where $\rho(n)$ controls the degree of pulse pressure variation (amplitude modulation), $y_c(n)$ is the quasi-periodic cardiac component,

$$y_c(n) = \sum_{k=1}^{N_c} a_c^2(k, n) \sin[k\theta_c(n) + \phi_c(k, n)] \quad (2)$$

and the quasi-periodic respiratory signal is modeled as,

$$y_r(n) = \sum_{k=1}^{N_r} a_r^2(k, n) \sin[k\theta_r(n) + \phi_r(k, n)] \quad (3)$$

If we assume that the phase components of the cardiac and respiratory harmonics, $\phi_c(k, n)$ and $\phi_r(k, n)$, are slowly varying, then the instantaneous respiratory and cardiac frequencies are given by

$$\omega(n) \triangleq \frac{d\theta(n)}{dn} \approx \frac{\theta(n+1) - \theta(n)}{T_s} \quad (4)$$

where $T_s = f_s^{-1}$ is the sampling interval. This can be expressed as a first-order difference equation

$$\theta(n+1) = \theta(n) + T_s s[\omega(n)] \quad (5)$$

TABLE I
LIST OF ALL MODEL PARAMETERS.

Name	Symbol	Number	Initial
Signal Trend	$m(n)$	1	$y(0)$
Cardiac Frequency	$\omega_c(n)$	1	$\bar{\omega}_c$
Respiratory Frequency	$\omega_r(n)$	1	$\bar{\omega}_r$
Cardiac Phase	$\theta_c(n)$	1	0
Respiratory Phase	$\theta_r(n)$	1	0
PPV Amplitude	$\rho(n)$	1	0
Cardiac Fundamental Amplitude	$a_{c,1}(n)$	N_c	0.5
Cardiac Harmonic Amplitudes	$a_{c,k}(n)$	N_c	0.1
Cardiac Harmonic Phases	$\phi_{c,k}(n)$	N_c	0
Respiratory Fundamental Amplitudes	$a_{r,k}(n)$	N_r	0.5
Respiratory Harmonic Amplitudes	$a_{r,k}(n)$	N_r	0.1
Respiratory Harmonic Phases	$\phi_{r,k}(n)$	N_r	0

where $\omega(n)$ is the instantaneous frequency in units of radians per sample and $s[\omega]$ is a saturation function that limits the range of the instantaneous frequency to known physiologic limits. In this paper we used a simple clipping function

$$s[\omega] = \begin{cases} \omega_{\min} & \omega < \omega_{\min} \\ \omega & \omega_{\min} \leq \omega \leq \omega_{\max} \\ \omega_{\max} & \omega_{\max} \leq \omega \end{cases} \quad (6)$$

This function improves the stability of the tracking algorithm and its robustness to common types of artifact.

We use a centered first-order autoregressive process model for the respiratory and cardiac frequencies

$$\omega_r(n+1) = \bar{\omega}_r + \alpha_r [\omega_r(n) - \bar{\omega}_r] + u_{\omega_r}(n) \quad (7)$$

$$\omega_c(n+1) = \bar{\omega}_c + \alpha_c [\omega_c(n) - \bar{\omega}_c] + u_{\omega_c}(n) \quad (8)$$

where $\bar{\omega}_r$ and $\bar{\omega}_c$ are a priori estimates of the expected respiratory rate provided by the user. The parameters α_r and α_c control the bandwidth of modeled variation about the mean frequencies. The instantaneous rates in units of Hz are then

$$f_r(n) = \frac{1}{2\pi T_s} s_r[\omega_r(n)] \quad (9)$$

$$f_c(n) = \frac{1}{2\pi T_s} s_c[\omega_c(n)] \quad (10)$$

B. Statistical Model of the Parameter Variation

The extended Kalman filter (EKF) is used to estimate the instantaneous cardiac and respiratory phases and frequencies. It also simultaneously estimates most of the model parameters listed Table I, which collectively comprise the system's state vector. As is common practice in parameter estimation problems that lack a natural statistical model for parameter variation, we used a random walk model of the form

$$x(n+1) = x(n) + u(n) \quad (11)$$

for all of the parameters, where $u(n)$ is a white noise process.

C. User-Specified Parameters

The user is responsible for specifying the fixed model parameters. Table II lists all of the user-specified parameters and the values that we used for the example given later.

TABLE II
USER-SPECIFIED PARAMETERS.

Name	Symbol	Value
Cardiac minimum frequency	$f_{c,\min}$	1.000 Hz
Cardiac mean frequency	\bar{f}_c	2.100 Hz
Cardiac maximum frequency	$f_{c,\max}$	3.000 Hz
Cardiac cutoff frequency	$f_{c,co}$	0.010 Hz
Cardiac harmonics	N_c	4
Cardiac frequency variance	$\sigma_{\omega_c}^2$	0.020 (rad/s) ²
Cardiac harmonic amplitude variance	$\sigma_{a_c}^2$	0.010 mmHg ²
Cardiac harmonic phase variance	$\sigma_{\phi_c}^2$	0.001 rad ²
Respiratory minimum frequency	$f_{r,\min}$	0.250 Hz
Respiratory mean frequency	\bar{f}_r	0.500 Hz
Respiratory maximum frequency	$f_{r,\max}$	0.700 Hz
Respiratory cutoff frequency	$f_{r,co}$	0.010 Hz
Respiratory harmonics	N_r	2
Cardiac frequency variance	$\sigma_{\omega_r}^2$	0.050 (rad/s) ²
Cardiac harmonic amplitude variance	$\sigma_{a_r}^2$	0.001 mmHg ²
Cardiac harmonic phase variance	$\sigma_{\phi_r}^2$	0.001 rad ²
Trend variance	σ_m^2	0.500 mmHg ²
PPV variance	σ_ρ^2	0.010

D. Extended Kalman Filter

The extended Kalman filter is a powerful algorithm that can estimate the state of a nonlinear state space model of the process given observations that are dependent on the state. Our nonlinear state space model can be expressed in the form

$$\mathbf{x}(n+1) = f[\mathbf{x}(n)] + \mathbf{u}(n) \quad (12)$$

$$\mathbf{y}(n) = h[\mathbf{x}(n)] + v(n) \quad (13)$$

where $h(\mathbf{x}_n)$ and $f(\mathbf{x}_n)$ are nonlinear functions of the l dimensional state vector \mathbf{x}_n , and $v(n)$ and \mathbf{u}_n are uncorrelated white noise processes with variances specified by the user (see Table II).

The extended Kalman filter and smoother are based on local linear approximations of the state-space model about an estimate of the state. Typically the linearization is only performed during the filter portion of the algorithm. The output is linearized about the predicted estimate $\hat{\mathbf{x}}(n|n-1)$, a prediction of the state at time n given only the preceding observations $\{\mathbf{y}(n-1), \dots, \mathbf{y}(0)\}$. The state prediction equation is linearized about the measurement update estimate $\hat{\mathbf{x}}(n|n)$, an estimate of the state given the current and preceding observations $\{\mathbf{y}(n), \dots, \mathbf{y}(0)\}$. The EKS estimates are obtained from the EKF estimates.

The extended Kalman filter recursions are as follows

$$H_n = \nabla_{\mathbf{x}} h(\mathbf{x})|_{\mathbf{x}=\hat{\mathbf{x}}(n|n-1)}$$

$$r_{e,n} = (H_n P_{n|n-1} H_n^T + r)$$

$$K_{f,n} = P_{n|n-1} H_n^T r_{e,n}^{-1}$$

$$e(n) = \mathbf{y}(n) - h[\hat{\mathbf{x}}(n|n-1)]$$

$$\hat{\mathbf{x}}(n|n) = \hat{\mathbf{x}}(n|n-1) + K_{f,n} e(n)$$

$$F_n = \nabla_{\mathbf{x}} f(\mathbf{x})|_{\mathbf{x}=\hat{\mathbf{x}}(n|n)}$$

$$\hat{\mathbf{x}}(n+1|n) = f[\hat{\mathbf{x}}(n|n)]$$

$$P_{n|n} = (I - K_{f,n} H_n) P_{n|n-1}$$

$$P_{n+1|n} = F_n P_{n|n} F_n^T + Q$$

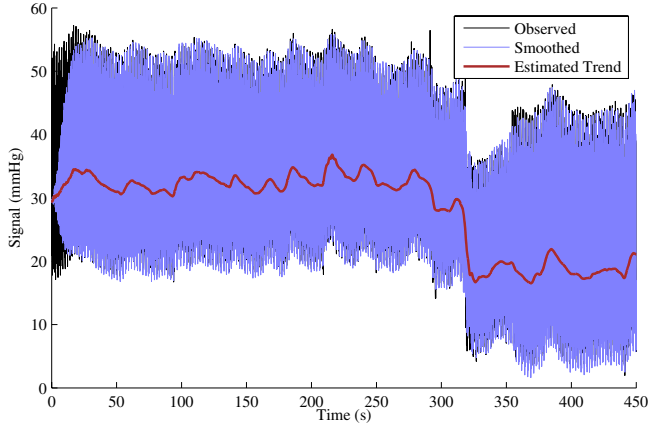


Fig. 1. Original ABP signal, the smoothed estimate, and the estimated trend $\hat{m}(n)$ over the course of the entire recording.

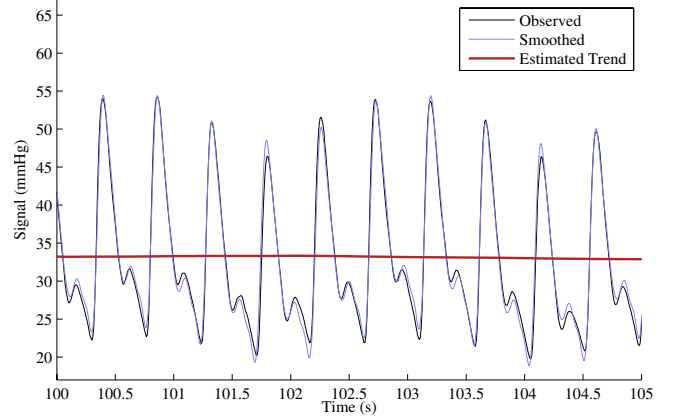


Fig. 2. Original ABP signal, the smoothed estimate, and the estimated trend $\hat{m}(n)$ over a 5 s segment of the signal.

where $\nabla_{\mathbf{x}} \triangleq \frac{\partial}{\partial \mathbf{x}}$ denotes the Jacobian operator. The algorithm requires an initial estimate of the state vector $\hat{\mathbf{x}}(0|-1)$ and the initial state covariance matrix $P_{0|-1}$. The initial values of the estimated state are listed in Table I. The initial state covariance was a diagonal matrix with 1% of the variance values listed in Table II.

E. Extended Kalman Smoother

There are many mathematically equivalent expressions for the extended Kalman smoother (EKS). Here we use a variant similar to that developed in [8] (see [9, p. 374]). The EKS is initialized with

$$\psi_{N+1|N} = 0 \quad (14)$$

where ψ is the adjoint variable. The smoothed estimates of the state variables can then be computed with the EKS as follows,

$$K_{p,n} = (F_n P_{n|n-1} H_n^T) r_{e,n}^{-1} \quad (15)$$

$$\psi_{n|N} = (F_n - K_{p,n} H_n)^T \psi_{n+1|N} + H_n^T r_{e,n}^{-1} e(n) \quad (16)$$

$$\hat{\mathbf{x}}(n|N) = \hat{\mathbf{x}}(n|n-1) + P_{n|n-1} \psi_{n|N} \quad (17)$$

III. ILLUSTRATIVE EXAMPLE

The following results show an illustrative example of the EKS applied to an ABP signal obtained from a sepsis patient. The (ABP) signal was acquired from a 22 or 24 gauge catheter connected to a Philips Merlin patient monitor in the pediatric intensive care unit at Doernbecher Children's Hospital. The sample rate was $f_s = 125$ Hz. The signal segment was 7.5 min in duration and contains an acute drop in pressure approximately 5.3 min into the recording.

Figs. 1 and 2 show the original observed signal, the estimated signal using the parameters estimated by the EKS, and the estimated trend. The predicted signal based on our proposed statistical model closely matches the real ABP signal after the initial transient. This indicates that both our proposed model for cardiac signals and the estimation algorithm are accurate.

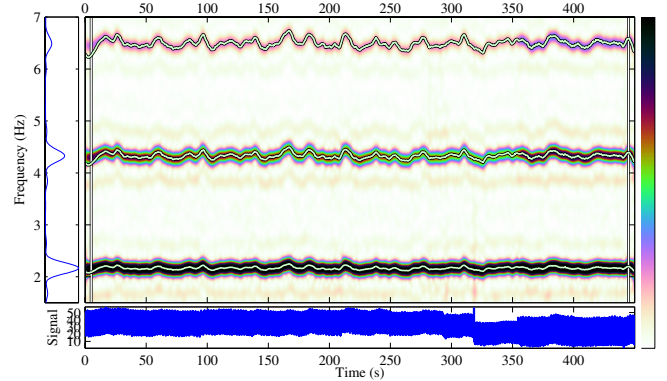


Fig. 3. Spectrogram of the ABP signal over a frequency range that shows the first three harmonics of the heart rate.

Fig. 3 shows a spectrogram of the ABP signal with the cardiac frequency estimated by the EKS overlaid. This example demonstrates that the estimator can accurately track the heart rate from the ABP signal. Similarly, Fig. 4 shows the estimated respiratory rate overlaid on top of the spectrogram. The second harmonic is quite faint in this case, but the EKS is able to track the respiratory rate accurately throughout most of the signal. The acute drop in pressure that occurred approximately 320 s into the recording caused the EKS to lose track of the respiratory rate. However, due to the clipping function that limits excursions of the estimated respiratory frequency, the EKS was able to regain track quickly. This demonstrates the robustness of the algorithm to artifact.

Figs. 5 and 6 show the phases and amplitudes of the cardiac and respiratory harmonics. As expected, both changed slowly.

Fig. 7 shows the EKS estimate of the PPV coefficient. This shows that $\rho(n)$, the ratio of the pulse pressure respiratory component to the additive respiratory component, was relatively stable at a value of approximately 0.035, except during the acute drop and the initial transient. Since the second

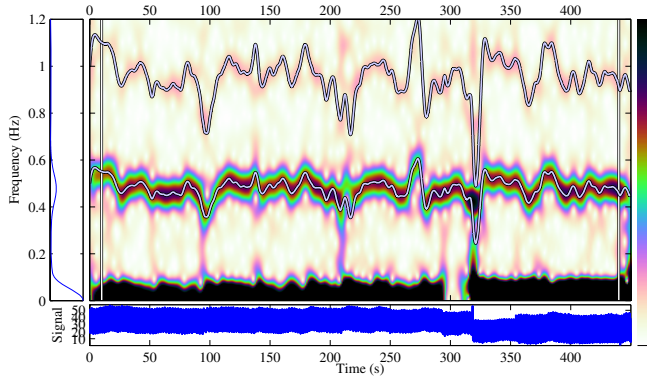


Fig. 4. Spectrogram of the ABP signal over a frequency range that shows the first two harmonics of respiration.

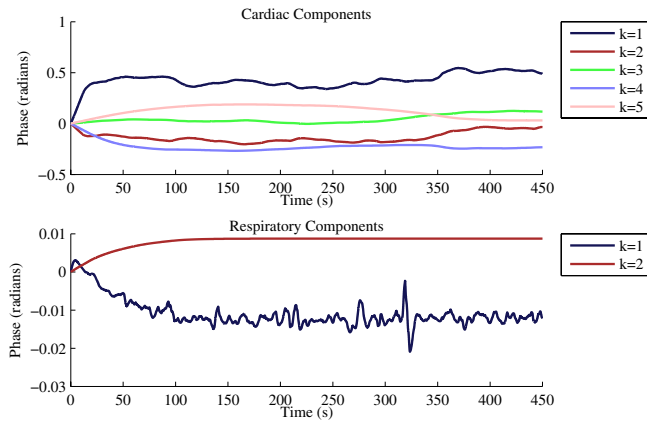


Fig. 5. Phases of the cardiac (top) and respiratory (bottom) harmonic components.

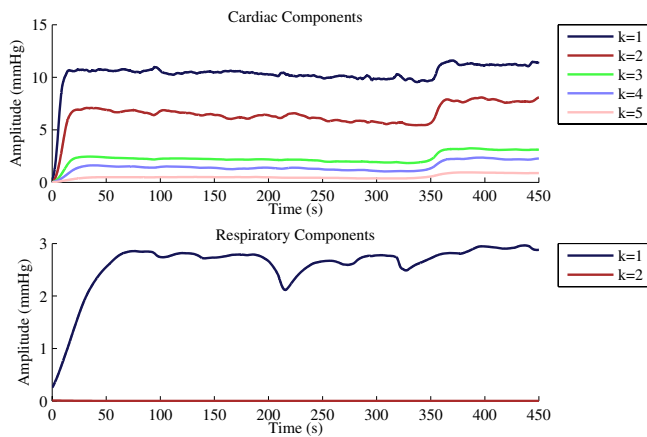


Fig. 6. Amplitudes of the cardiac (top) and respiratory (bottom) harmonic components.

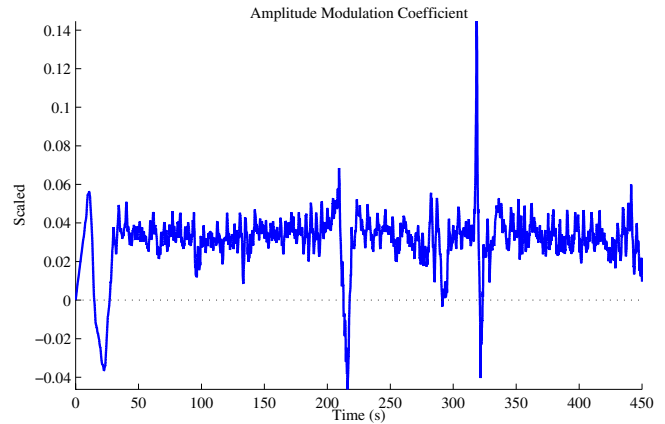


Fig. 7. Amplitude modulation coefficient (ρ).

respiratory harmonic had a small amplitude, the actual pulse pressure variation was approximately $2a_1^2(1, n)\rho(n) \approx 55\%$ throughout the record.

IV. CONCLUSION

We proposed a novel statistical state space model for cardiovascular signals such as ABP, S_pO_2 , and CVP. We used extended Kalman filter and smoother to accurately estimate and track all of the significant components of the signals. An illustrative example demonstrated the versatility, accuracy, and robustness of the algorithm to artifact.

REFERENCES

- [1] F. Michard, S. Boussat, D. Chemla, N. Anguel, A. Mercat, Y. Lecarpentier, C. Richard, M. R. Pinsky, and J. L. Teboul, "Relation between respiratory changes in arterial pulse pressure and fluid responsiveness in septic patients with acute circulatory failure." *Am J Respir Crit Care Med*, vol. 162, no. 1, pp. 134–8, Jul 2000.
- [2] F. Michard, L. Ruscio, and J. L. Teboul, "Clinical prediction of fluid responsiveness in acute circulatory failure related to sepsis." *Intensive Care Med*, vol. 27, no. 7, p. 1238, Jul 2001.
- [3] A. Kramer, D. Zygun, H. Hawes, P. Easton, and A. Ferland, "Pulse pressure variation predicts fluid responsiveness following coronary artery bypass surgery." *Chest*, vol. 126, no. 5, pp. 1563–8, Nov 2004.
- [4] F. Michard, "Changes in arterial pressure during mechanical ventilation." *Anesthesiology*, vol. 103, no. 2, pp. 419–28; quiz 449–5, Aug 2005.
- [5] C. K. Hofer, L. Furrer, S. Matter-Ensner, M. Maloigne, R. Klaghofer, M. Genoni, and A. Zollinger, "Volumetric preload measurement by thermodilution: a comparison with transoesophageal echocardiography." *Br J Anaesth*, vol. 94, no. 6, pp. 748–55, Jun 2005.
- [6] M. Aboy, J. McNames, T. Thong, C. R. Phillips, M. S. Ellenby, and B. Goldstein, "A novel algorithm to estimate the pulse pressure variation index deltaPP." *IEEE Trans Biomed Eng*, vol. 51, no. 12, pp. 2198–203, Dec 2004.
- [7] R. Kalman, "A new approach to linear filtering and prediction problems," *Transactions of the ASME—Journal of Basic Engineering*, vol. 82, no. Series D, pp. 35–45, 1960.
- [8] A. E. Bryson and M. Frazier, "Smoothing for linear and nonlinear dynamic systems," Aero. Sys. Div. Wright-Patterson Air Force Base, Ohio, Tech. Rep. TDR 63-119, 1963.
- [9] T. Kailath, A. H. Sayed, and B. Hassibi, *Linear Estimation*. Prentice Hall, 2000.